



Evolution of structure and electrical properties with annealing time in solution-based VO₂ thin films



Yuxian Guo^{a,*}, Haiyan Xu^b, Chongwen Zou^{c,*}, Zhiyun Yang^a, Bin Tong^b, Jiangying Yu^a, Youjie Zhang^a, Li Zhao^a, Yaling Wang^a

^a School of Mathematics & Physics, Anhui Jianzhu University, Hefei 230022, Anhui, PR China

^b School of Materials & Chemical Engineering, Anhui Jianzhu University, Hefei 230022, Anhui, PR China

^c National Synchrotron Radiation Laboratory, University of Science and Technology of China, Hefei 230029, Anhui, PR China

ARTICLE INFO

Article history:

Received 29 August 2014

Received in revised form 27 October 2014

Accepted 3 November 2014

Available online 11 November 2014

Keywords:

Vanadium oxide

Sol–gel method

Vacuum annealing

Annealing time

ABSTRACT

Vanadium dioxide (VO₂) thin films were prepared on c-sapphire substrates by using an easy sol–gel method and sequential vacuum annealing process. The effects of annealing time on the structure, morphology and phase transition properties were investigated. The results show that, with the extended annealing time from 1 h to 7 h, the films have transformed from V₂O₃ to V₃O₅, and then VO₂. The VO₂ thin films prepared with the annealing time of 4 h or 7 h display good phase transition property with the resistance change up to 3 orders of magnitude. Furthermore, the 7 h-sintered film has better growth orient, bigger grain size and lower phase transition temperature comparing with the 4 h-sintered film. It is suggested that, the prolonged annealing treatment will be in favor of the crystal film quality and enhance the related phase transition property for the solution-based VO₂ films. Based on the Raman results, we have discussed the possible reactions and evolution mechanisms during the VO₂ film preparation with different annealing time.

© 2014 Elsevier B.V. All rights reserved.

1. Introduction

It is well known that VO₂ films undergo a metal–insulator transition (MIT) at a critical temperature (T_c) close to room temperature, accompanied by abrupt variations in electrical resistivity, optical transmittance, and reflectance in the infrared region [1–3]. These properties make them suitable for technological applications such as smart windows, temperature sensors, gas molecule sensors, solid-state battery cathode, electrical and optical switching devices [4–6].

Up to now, various methods such as chemical deposition, pulse laser deposition and magnetron sputter [7–11], have been employed for preparing VO₂ thin films. Among them, the sol–gel method has been proved to be one of the most convenient routes to synthesize VO₂ thin films, if considering the advantages such as low cost, large area deposition, and feasibility of metal-doping [12,13]. However, it is very difficult to obtain highly oriented VO₂ thin films by using the sol–gel method, due to the multi-valence state of V ions and the various VO₂ phase structures [12]. During the VO₂ preparation by sol–gel, the annealing parameters,

including the vacuum pressure, annealing time and heating rate, are crucial for the quality of the film and the final vanadium valence state. Among them, the annealing time has a remarkable effect on the crystalline structure, the morphology and the grain size distribution, which further effects the phase transition properties of the prepared VO₂ films. It is reported that VO₂ thin films can be prepared by the reduction of V₂O₅. For example, Wang et al. [14] synthesized VO₂ thin films by post-annealing treatment in a vacuum environment of 1.2×10^{-4} Pa and an annealing temperature of 750 °C; while Wang et al. [15] obtained VO₂ films in a vacuum pressure of 10^{-2} Pa and an annealing temperature between 420 °C and 500 °C. For these cases, the experimental vacuum pressure is quite high and the Turbo molecular pump is always needed for the annealing system, which seriously limits their applications. In the recent study, we have prepared VO₂ films at a rougher vacuum of ~ 5 Pa with a simple vacuum pump [16], and found that the vanadium valence state were closely associated with the process parameters. Meanwhile, we proposed a self-reduction reaction mechanism for the vanadium oxide formation, which indicated that the reducer came from the decomposition of the original precursors. However, up to our knowledge, the systematic investigation about the annealing time influence on the structural and phase transition properties of VO₂ thin films is still not

* Corresponding authors. Tel.: +86 551 63828134; fax: +86 551 63828133.

E-mail addresses: guo_yuxian@163.com (Y. Guo), czou@ustc.edu.cn (C. Zou).

documented in the literatures. The reaction mechanism, especially for the annealing treatment in a low vacuum condition, still needs further experimental investigations.

In this study, VO₂ thin films have been prepared by sol-gel method at a low annealing temperature of 430 °C. The results show that the annealing time has a significant influence on the crystal structure, the morphology and the grain size, which further impacts their phase transition properties. Furthermore, the proposed self-reduction reaction mechanism for the VO₂ film preparation during the annealing process is experimentally revealed by the related Raman results.

2. Experimental

VO₂ thin films were grown on Al₂O₃(0001) substrates by using a sol-gel method and sequential annealing process, similar to previous publication [16]. Initially, the vanadyl triisopropoxide (VO(OC₃H₇)₃) was dissolved in isopropanol after vigorous stirring to form a uniform solution with the concentration of 0.12 M, and the films were spin-coated on Al₂O₃(0001) substrates at 200 rpm for 5 s and 2000 rpm for another 20 s. Then the coated films were dried at 250 °C in air for 3 min to drive off the excess solvent, forming the VO_x precursor films. The further reduction to V⁴⁺ could be only achieved by the subsequent annealing in a tube furnace at 430 °C for various annealing times with a rough vacuum atmosphere (~5 Pa). After the annealing treatment, the obtained precursor gel films were finally crystallized into VO₂. The average thickness of films was measured to be about 50 nm by using spectroscopic ellipsometry at room temperature.

The crystalline structure of the film samples were characterized by an X-ray diffractometer (XRD, Cu K_α, Rigaku D/MAX2500V). The Raman spectra were recorded at room temperature by using a confocal-microscope Raman spectrometer (Ar⁺ laser, 514.5 nm, LabRAM HR) with a spectral resolution of about 2 cm⁻¹. The surface morphologies and the particle structures of the films were investigated by atomic force microscopy (AFM, CSPM4000). The temperature-dependent resistance (*R-T* curve) was measured by a home-made four-probe measurement system with a variable temperature sample stage.

3. Results and discussion

3.1. Results of XRD measurements

Fig 1 shows the θ - 2θ XRD patterns of the VO₂ thin films deposited on c-sapphire with different annealing time of 1 h, 2 h, 4 h, 7 h, respectively. Besides the Al₂O₃(0006) substrate peak, all films have only one or two diffraction peaks, showing preferred oriented growth. It is observed that after 1 h of annealing at 430 °C, the precursor gel film is transformed to V₂O₃ compound with a (006) diffraction peak located at 38.8°. As the annealing time is prolonged to 2 h, the peak of V₃O₅($\bar{3}12$) appears instead of V₂O₃(006); while a weak peak of VO₂(020) is also observed at $2\theta = 39.8^\circ$, indicating the formation of VO₂ compound. When the annealing time is up to 4 h, a well (020) oriented VO₂ crystal

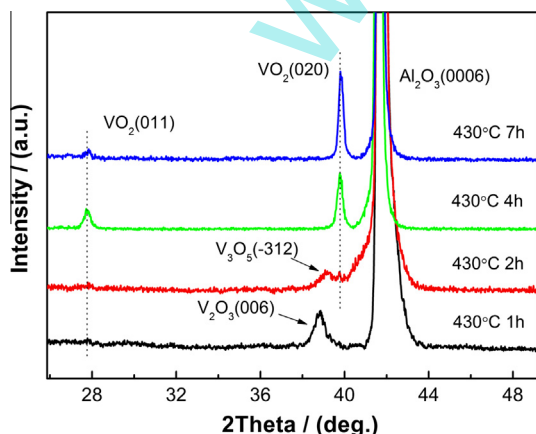


Fig. 1. XRD patterns of VO₂ films grown on Al₂O₃(0001) substrates with different annealing times.

emerges, and a weak VO₂(011) diffraction located at 27.8° is also observed. As the annealing time is further extended to 7 h, the VO₂(020) peak becomes more distinct and stronger while the VO₂(011) peak is weaker than that of the 4 h-sintered film, indicating that the 7 h-sintered film has a further improved crystalline with the (020) growth orientation.

To examine the variations of grain sizes with annealing time, we analyzed the diffraction peak position and FWHM by Gauss fitting, and calculated the grain sizes by using the Scherrer's equation. The results show that, with the varied annealing time from 1 h to 7 h, the grain sizes are about 15 nm, 7 nm, 29 nm, 33 nm, respectively. The FWHM of (020) peak for 7 h-sintered film is only 0.25°, indicating a high crystalline quality. According to Brassard's report [17], the grain size has a direct correlation with its MIT property. The corresponding influence will be specifically discussed in subsequent analysis.

3.2. Surface morphology

Fig. 2 shows the AFM images of prepared specimens with various annealing time. It can be seen that, the annealing time has a great influence on the surface morphology and microstructure of the films. As shown in Fig. 2(a), the 1 h-sintered film has some aligned stripes and grooves formed on the surface, which should be mainly resulted from the spin-coating process. In addition, there are no obvious particle structure to be found, suggesting that the film is mainly composed of some amorphous substance, which is consistent with smaller grain size of V₂O₃ from XRD. When the annealing time is prolonged to 2 h in Fig. 2(b), the stripe-shaped grooves disappear and the film surface becomes much flatter. The surface roughness of 2 h-sintered film is measured to be about 2.5 nm, indicating the prolonged annealing time can effectively smooth the film surface. It should be noticed that the particle structure of 2 h-sintered film is still not clear, which may be associated with the chemical reaction occurred inside the film sample. This chemical reaction is also reflected by the variation of the diffraction peak location from XRD measurements. As the annealing time is further extended to 4 h (Fig. 2(c)), we can observe some clear and dense grains structure, corresponding to the presence of VO₂ formation, which is confirmed from the clear (020) diffraction peak from XRD. From this graph, the particle size can be measured to be about 95 nm, which is larger than the obtained value (29 nm) from XRD, suggesting that the small nano-crystals are agglomerated together to form larger particles. Thus the observed particles on the sample surface from AFM images are actually composed of several small grains.

Finally, when the annealing time is prolonged from 4 h to 7 h (Fig. 2(d)), the mean particle size is increased from 95 nm to 153 nm, suggesting that longer annealing time favor the formation of larger particles. The particle sizes from AFM is larger than that from XRD result by Scherrer's equation, indicating that the overall particle size measured by AFM shows the grains agglomeration whereas XRD measurement only gives an mean grain size. The above phenomena can be explained as follows: firstly, for the annealing time of 4 h, the diffusion of atoms is encouraged and the atoms of vanadium and oxygen react sufficiently to form VO₂ compound. As the film was annealed with much longer annealing time of 7 h, the recombination of VO₂ molecules makes the composition in partial area relatively uniform during thermal diffusion, resulting in the larger particle sizes of thin films.

3.3. Raman measurements

Fig. 3 shows the Raman spectra of films with various annealing time of 1 h, 2 h, 4 h, and 7 h, respectively. It can be seen that, the films with annealing times of 4 h and 7 h have good M-VO₂ Raman

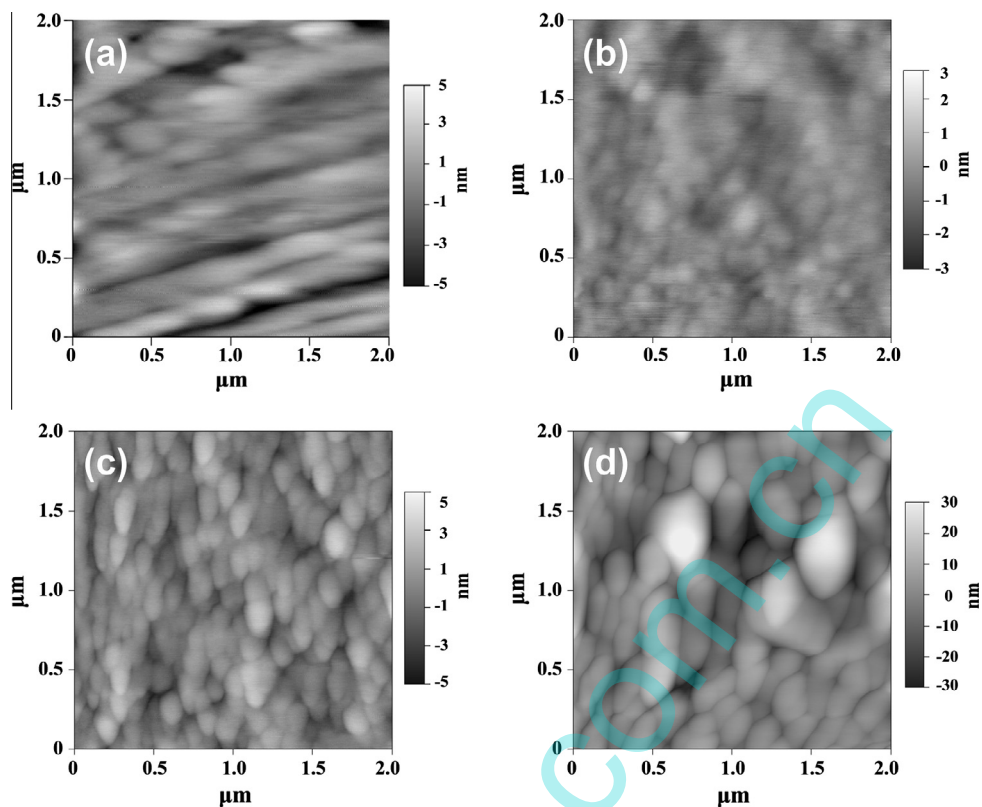


Fig. 2. Topographic AFM ($2 \times 2 \mu\text{m}$) of VO_x samples annealed under vacuum pressure of $\sim 5 \text{ Pa}$ at $430 \text{ }^\circ\text{C}$ with annealing times of 1 h (a), 2 h (b), 4 h (c) and 7 h (d), respectively.

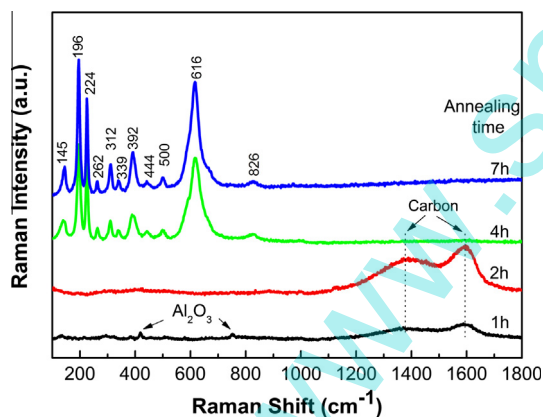


Fig. 3. Raman spectra for films with various annealing times of 1 h, 2 h, 4 h, 7 h, respectively. The Raman shifts for M-VO_2 are marked with numbers, and those for carbon and Al_2O_3 are marked with arrows as well.

modes. The corresponding peaks are centered at 145, 196, 224, 262, 312, 339, 392, 444, 500, 616, and 826 cm^{-1} , respectively, which is consistent with previous literatures [18,19]. Here the measurement accuracy of Raman shifts is about $\pm 2 \text{ cm}^{-1}$. Furthermore, besides the above-described VO_2 peaks, no other vanadium oxides such as V_2O_3 and V_2O_5 are detected, indicating that the crystal phase for the obtained specimens is quite pure. In comparison, the film with annealing time of 7 h has sharper peaks than that of 4 h, indicating that prolonged annealing time is more favorable for the crystallization of VO_2 films.

It is also observed that, there are no sharp and obvious peaks in Raman spectra for the samples sintered within 1 h and 2 h, which may be associated with the metal property of these films at room

temperature. In addition, two significant shifts located at 1386 and 1598 cm^{-1} are observed, which are usually attributed to the vibration of carbon atoms with dangling bond for the in-plane terminated disordered graphite [20,21]. The appearance of these two Raman shifts indicates the presence of a certain amount of carbon in the films, which is ascribed to the decomposition of the $(\text{VO}(\text{OC}_3\text{H}_7)_3)_3$ precursor. With the extending of annealing time to 4 h and then 7 h, the signal of carbon disappears and the crystallized VO_2 films are obtained. This result strongly support the self-reduction mechanism proposed in our previous report [16], and the presence of V^{3+} in XRD experiment is satisfactorily explained. Typically, the precursor containing V^{5+} can be reduced to V^{4+} at the vacuum degree of 10^{-2} Pa [15]. But, in this work, the highly oriented VO_2 films can be obtained at vacuum degree of $\sim 5 \text{ Pa}$, indicating that this reduction mechanism is beneficial for reducing the vacuum requirements during the annealing process.

In addition, for the 1 h-sintered film two weak peaks located at 419 and 752 cm^{-1} are observed, which corresponds to the signal of Al_2O_3 substrate according to Wu's report [18]. The appearance of this signal can be explained that, the surface grooves confirmed by AFM make the substrate signals easy to be detected. However, when the annealing time is prolonged to 2 h, the surface grooves are effectively repair and the film became flat, thus the Raman signal from substrate are absent.

3.4. Temperature-dependent resistance measurement

Fig. 4 shows the electrical property of VO_2 films as the function of temperature. Regardless of their high crystallinity shown in XRD data, the resistance curves of the films with the annealing time of 4 h and 7 h show obvious hysteresis properties, and the resistance changes across the phase transition is over three orders of magnitude. In general, for monoclinic VO_2 films, the semiconductor

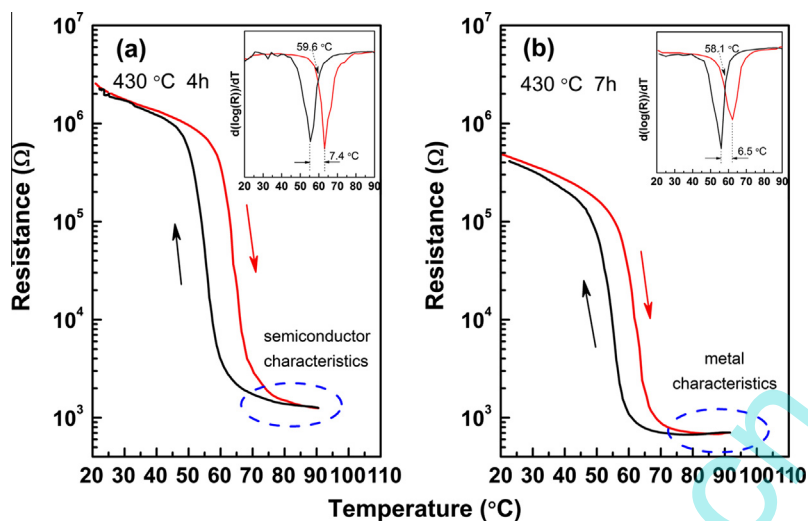


Fig. 4. (a) The temperature dependence of electrical resistance for the VO₂ films prepared with annealing times of (a) 4 h and (b) 7 h. The corresponding differential curves of both heating and cooling segment are shown on the insets.

characteristics at low temperature leads to the electrical resistance decreases exponentially with the rising temperature; while the metal characteristics at high temperature side results in the linear increase of resistance as the temperature rises. The prepared film with annealing time of 7 h is exactly in line with the above case, showing a metal characteristics in high temperature side. Thus it is verified that we do have prepared a single-phase VO₂. While the resistance for the 4 h-sintered film reduces with the drop of temperature at the high temperature side, similar to the resistance characteristics of a semiconductor, indicating the film contains a small amount of V⁵⁺ (e.g. V₂O₅). For this case, the resistance change with temperature exhibits semiconductor characteristics, which would affect the resistance variation for M-VO₂. Since there are no other vanadium oxides, expect VO₂, in the 4 h-sintered VO₂ films from the XRD or Raman spectra, we can speculate that some amorphous V⁵⁺ species existed in the films. Though the amount of V⁵⁺ species is quite tiny, it still has a considerable effect on the electrical properties of the 4 h-sintered VO₂ films. According to previous reports [22,23], the content of V⁵⁺ may be derived from surface oxidization either in the annealing process or during storage in air. The fact that 4 h-sintered film is more easily oxidized should be related to its smaller particle size confirmed by AFM measurements.

In order to facilitate further comparisons, the differential log₁₀R–T curves are also displayed in the inset of Fig. 4, and two main differences are found. Firstly, the T_c values for both films are 59.6 °C and 58.1 °C, which is much lower than the corresponding bulk value (68 °C) of VO₂. The reason can be explained as the following. The VO₂ obtained at the current annealing conditions (5 Pa, 430 °C) is in a hypoxic state, e.g. V:O > 1:2, which leads to the appearance of oxygen vacancies and increases the concentration of V³⁺. According previous reports [24], these extra electrons induced by V³⁺ in films would decrease the π* bands level and reduce the gap, resulting in the drop of T_c. In comparison, the 7 h-sintered film has lower T_c than 4 h-sintered film. Combined with the results of XRD and AFM, we believe that the higher grain orientation and distinct aggregation lead to the propagation of phase transition between grains becomes easier, reducing the value of T_c in a limited degree. Second, the transition width for the 7 h-sintered film is 6.5 °C, lower than that for the 4 h-sintered film (7.4 °C). According to the literatures [25,26], the transition width is related to the degree of oriented crystallization (or misorientation between adjacent grains), and grain size. Thus we

speculate that, the fact that the film with 7 h annealing corresponds to narrower transition width are basically resulted from the larger grain size and better growth orientation confirmed by XRD.

4. Conclusions

In conclusion, we have studied the effect of annealing time on the structural and phase transition properties for VO₂ thin films by sol–gel method. As the annealing time is prolonging from 1 h to 7 h, the films has transformed from V₂O₃ to V₃O₅, and then VO₂. Both the V₂O₃ and V₃O₅ thin films, with annealing time of 1 h and 2 h respectively, display small crystalline sizes of 15 nm and 7 nm; while the thin films of VO₂ prepared with 4 h and 7 h show good phase transition property, with the resistance changes up to three orders of magnitude, phase transition width of 7.4 °C and 6.5 °C respectively. It is suggested that prolonged annealing time is beneficial for the formation of VO₂ films with better growth orientation, larger grain size and smaller transition width.

Acknowledgments

This work is partially supported by the National Natural Science Foundation of China (11175183 and 21271007), the Anhui Provincial Natural Science Foundation (1408085MA17) and the Open Fund (LABKF1401) of the State Key Laboratory of Materials Modification by Laser, Ion and Electron Beams in Dalian University of Technology, China.

References

- [1] T.-H. Yang, R. Aggarwal, A. Gupta, H. Zhou, R.J. Narayan, J. Narayan, *J. Appl. Phys.* 107 (5) (2010) 053514.
- [2] G.J. Kovacs, D. Buerger, I. Skorupa, H. Reuther, R. Heller, H. Schmidt, *J. Appl. Phys.* 109 (6) (2011) 5.
- [3] L. Whittaker, T.L. Wu, C.J. Patridge, G. Sambandamurthy, S. Banerjee, *J. Mater. Chem.* 21 (15) (2011) 5580–5592.
- [4] M. Soltani, M. Chaker, E. Haddad, R.V. Kruzelesky, *J. Vac. Sci. Technol., A* 24 (3) (2006) 612–617.
- [5] W. Burkhardt, T. Christmann, S. Franke, W. Kriegseis, D. Meister, B.K. Meyer, W. Niessner, D. Schalch, A. Scharmann, *Thin Solid Films* 402 (1–2) (2002) 226–231.
- [6] H. Jerominek, F. Picard, D. Vincent, *Opt. Eng.* 32 (9) (1993) 2092–2099.
- [7] B.G. Chae, H.T. Kim, S.J. Yun, B.J. Kim, Y.W. Lee, D.H. Youn, K.Y. Kang, *Electrochem. Solid State Lett.* 9 (1) (2006) C12–C14.

- [8] L.L. Fan, Y.F. Wu, C. Si, C.W. Zou, Z.M. Qi, L.B. Li, G.Q. Pan, Z.Y. Wu, *Thin Solid Films* 520 (19) (2012) 6124–6129.
- [9] P. Pfalzer, G. Obermeier, M. Klemm, S. Horn, M.L. denBoer, *Phys. Rev. B* 73 (14) (2006) 144106.
- [10] M.M. Qazilbash, A.A. Schafgans, K.S. Burch, S.J. Yun, B.G. Chae, B.J. Kim, H.T. Kim, D.N. Basov, *Phys. Rev. B* 77 (11) (2008) 115121.
- [11] D. Vernardou, M.E. Pemble, D.W. Sheel, *Surf. Coat. Technol.* 188 (2004) 250–254.
- [12] N.Y. Yuan, J.H. Li, C.L. Lin, *Appl. Surf. Sci.* 191 (2002) 176–180.
- [13] B.G. Chae, H.T. Kim, *Phys. B-Condens. Matter* 405 (2) (2010) 663–667.
- [14] N. Wang, S. Magdassi, D. Mandler, Y. Long, *Thin Solid Films* 534 (2013) 594–598.
- [15] Y.L. Wang, M.C. Li, L.C. Zhao, *Surf. Coat. Technol.* 201 (15) (2007) 6772–6776.
- [16] Y. Guo, C. Zou, Y. Liu, Y. Xu, X. Wang, J. Yu, Z. Yang, F. Zhang, R. Zhou, *J. Sol–Gel Sci. Technol.* 70 (2014) 40–46.
- [17] D. Brassard, S. Fourmaux, M. Jean-Jacques, J.C. Kieffer, M.A. El Khakani, *Appl. Phys. Lett.* 87 (5) (2005) 051910.
- [18] Y.F. Wu, L.L. Fan, S.M. Chen, S. Chen, C.W. Zou, Z.Y. Wu, *AIP Advances* 3 (4) (2013) 042132.
- [19] J.M. Wu, L.B. Liou, *J. Mater. Chem.* 21 (14) (2011) 5499–5504.
- [20] A.C. Ferrari, J. Robertson, *Phys. Rev. B* 61 (20) (2000) 14095–14107.
- [21] V.G. Pol, S.V. Pol, J.M. Calderon-Moreno, A. Gedanken, *J. Phys. Chem. C* 113 (24) (2009) 10500–10504.
- [22] T.D. Manning, I.P. Parkin, M.E. Pemble, D. Sheel, D. Vernardou, *Chem. Mater.* 16 (4) (2004) 744–749.
- [23] R. Lindström, V. Maurice, S. Zanna, L. Klein, H. Groult, L. Perrigaud, C. Cohen, P. Marcus, *Surf. Interface Anal.* 38 (1) (2006) 6–18.
- [24] A. Zylbersztein, N.F. Mott, *Phys. Rev. B* 11 (11) (1975) 4383–4395.
- [25] D.H. Kim, H.S. Kwok, *Appl. Phys. Lett.* 65 (25) (1994) 3188.
- [26] J.F. Denatale, P.J. Hood, A.B. Harker, *J. Appl. Phys.* 66 (12) (1989) 5844–5850.